

## Resonance analysis in pp collisions with the ALICE detector

A. PULVIRENTI(\*) for the ALICE COLLABORATION

*INFN, Sezione di Catania - Catania, Italy*  
*Università di Catania - Catania, Italy*

(ricevuto il 27 Gennaio 2011; approvato il 28 Gennaio 2011; pubblicato online il 30 Marzo 2011)

**Summary.** — ALICE is the LHC experiment mainly dedicated to the study of hot and high energy density QCD matter created in heavy-ion collisions. It has also developed a detailed proton-proton physics programme, in order to exploit its capabilities to investigate the novel energy regime made available by LHC, which turns out to be quite interesting in itself besides being important as a baseline for the heavy-ion data. Results will be presented of the first resonance measurements done on the data taken at LHC during 2009 and 2010, in pp collisions at 900 GeV and 7 TeV center-of-mass energy.

PACS 25.75.Nq – Quark deconfinement, quark-gluon plasma production, and phase transitions.

PACS 25.75.Gz – Particle correlations and fluctuations.

PACS 14.20.Jn – Hyperons.

PACS 14.40.-n – Mesons.

### 1. – Introduction

The study of identified particle production in pp collisions provides a fundamental baseline for properly tuning the QCD-inspired models in order to make predictions at higher energies. In the low- $p_T$  region this helps especially in understanding the nature of the soft part of the underlying event. The ALICE detector [1], thanks to its low operating magnetic field (0.5 T) and to its excellent particle identification (PID) capabilities, is well suited for the study of low- $p_T$  particle production at mid-rapidity.

Studying the hadronic resonances in pp collisions, besides contributing to this topic, provides also a baseline for a better understanding of heavy-ion collisions, where they are useful probes to estimate the lifetime of the fireball created there (for a summary about this topic, see [2, 3] and references therein).

---

(\*) E-mail: [alberto.pulvirenti@ct.infn.it](mailto:alberto.pulvirenti@ct.infn.it)

Several resonances were analysed in the first LHC pp runs, taken between the end of 2009 and the first half of 2010, respectively at the energies of 900 GeV and 7 TeV. Section 2 briefly illustrates the most important aspects of the ALICE detector exploited for these studies. Section 3 presents in more detail the analysis carried on the  $\phi(1020)$  resonance with the first 2009 runs at 900 GeV. Section 4 shows some preliminary results in the analysis of  $K^*(892)^0$ ,  $\Sigma(1385)$  and  $\phi(1020)$  resonances with the pp collisions at 7 TeV. Finally, in sect. 5 conclusions are given.

## 2. – Experimental setup

ALICE is the LHC experiment most specifically devoted to the study of heavy-ion collisions. It is designed to guarantee a complete reconstruction and identification of the particles produced in those collisions (for details about the detector, see [1]).

The combination of several detectors is used in this analysis. Charged particles are tracked in the Time Projection Chamber (TPC) and in the Inner Tracking System (ITS). The Silicon Pixel Detectors (SPD) in the two innermost ITS layers also contribute to the primary vertex reconstruction. Both the TPC and the ITS give a  $dE/dx$  measurement which can be used for particle identification (PID). At larger momenta (above  $\sim 0.7$  GeV/ $c$ ) the Time-of-Flight detector (TOF) is also used for PID.

At the trigger level two VZERO scintillator counters displaced around the beam line allow one to reject most of the beam-gas interactions, in order to have an initial hardware-level minimum bias event selection. This is then refined offline by means of a check on trigger masks, in order to accept only the events collected by the two V0 triggers and those coming from the SPD. Moreover, all events with longitudinal primary vertex position  $Z_V \geq 10$  cm are rejected in order to avoid biases due to the detector acceptance.

## 3. – $\phi(1020)$ analysis with LHC commissioning runs in 2009

**3.1. Track selection.** – The  $\phi$  resonance was reconstructed through its  $K^+K^-$  decay channel (BR 49.2%). For major details, see [4].

Tracks used for this analysis are required to have been reconstructed by both TPC and ITS, with at least 80 clusters in the TPC and a total  $\chi^2$  (normalized to the number of TPC points) smaller than 4, in order to ensure a good track quality. Since resonance daughters are indistinguishable from primaries, tracks were also required to have a distance of closest approach to primary vertex smaller than 0.5 cm (3 cm) in the transverse (longitudinal) direction.

A PID request was also made, in the form of a “compatibility cut” both in TPC and TOF. First of all, the track  $dE/dx$  measured in the TPC is required to stay within a  $3\sigma_{TPC}$  ( $5\sigma_{TPC}$ ) band around the Bethe-Bloch curve computed with a kaon hypothesis. The state of the art of the TPC calibration for the analyzed sample allowed one to assume a resolution  $\sigma_{TPC} = 6\%$ . When the track has a matched cluster in the TOF, an additional check is done on the difference between the time of flight measured by the TOF and that calculated for a kaon with the same momentum. In this case, the fiducial band is defined by two momentum-dependent hyperbolas, as is shown in fig. 1 (right), to cope with the worsening TOF resolution at small momenta (for  $p_T \leq 260$  MeV/ $c$  the TOF is never used). Since the TPC-TOF matching efficiency is almost 60%, whenever a TOF signal is absent in the track, the TPC PID condition only is used.

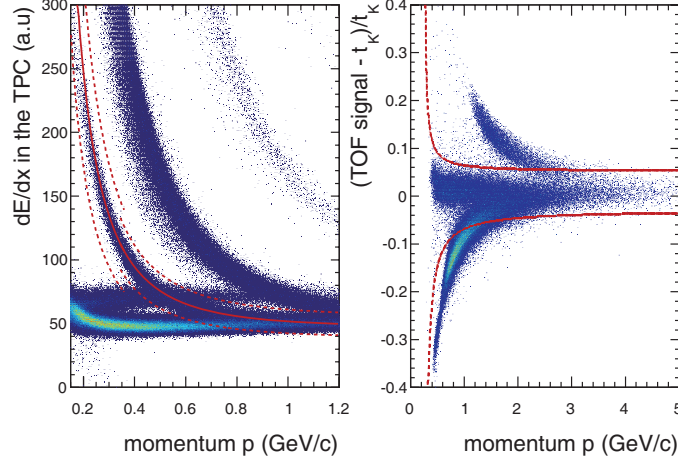


Fig. 1. – (Left) TPC signal *vs.* total momentum at the inner TPC wall. The central continuous curve is the Bethe-Bloch parameterization, and the two broken curves define the  $3\sigma_{TPC}$  and  $5\sigma_{TPC}$  bands used for the compatibility condition. (Right) The relative difference between the time of flight measured by the TOF and that of a kaon with the same momentum; the curves define the fiducial window.

**3.2. Signal extraction and correction.** – The measurement was done in four  $p_T$  bins between 0.7 and 3 GeV/c and in a rapidity window  $|y| \leq 0.6$ , where the efficiency was found to be almost flat. An invariant mass distribution was computed with all unlike-sign charged track pairs (see fig. 2, left) and fitted with a square-root function ( $A\sqrt{m - m_0}$ ) plus a Gaussian, to reproduce the peak plus the background. Then, the number of  $\phi$  was computed from the number of entries in the invariant mass range  $m_\phi \pm 4\sigma$ , where  $\sigma = \Gamma_\phi/2.35$  and  $m_\phi$  and  $\Gamma_\phi$  are the PDG nominal mass and width of this resonance, minus the integral of background function computed in the same range.

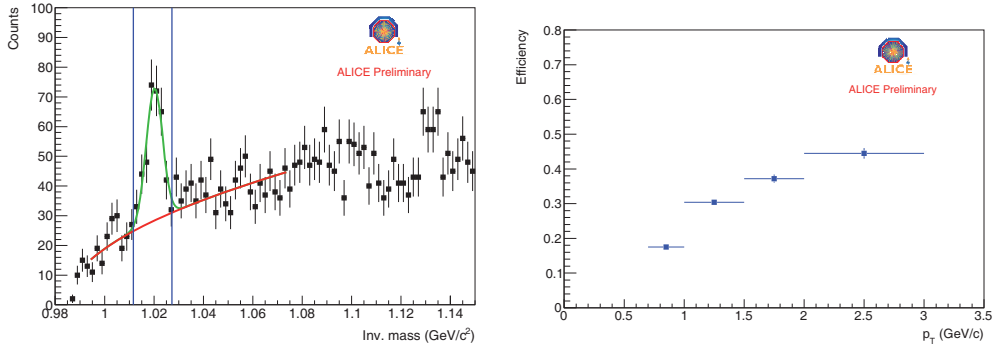


Fig. 2. – (Left)  $K^+K^-$  invariant mass spectrum in the  $p_T$  bin between 1 and 1.5 GeV/c. The curve is the combined fit of square-root function + Gaussian, and the vertical lines delimit the region where the subtraction is computed. (Right) Efficiency of reconstructed  $\phi$  computed in the PYTHIA sample cited in the text, in the four measured  $p_T$  bins (branching ratio not included).

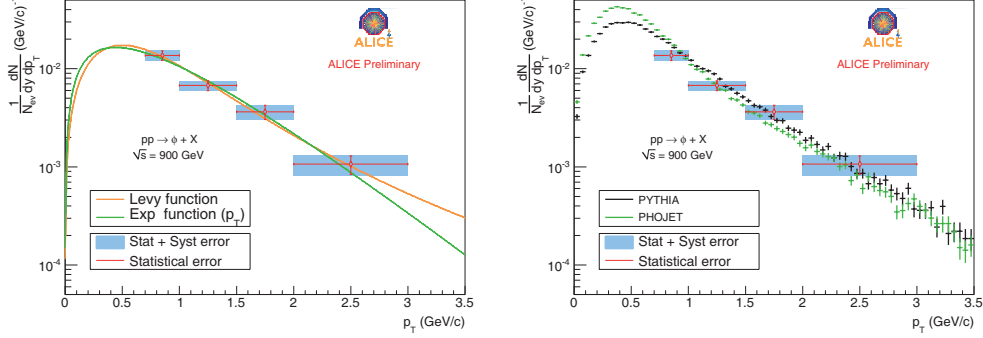


Fig. 3. – (Left) Corrected  $\phi$  spectrum as a function of  $p_T$ . Shaded boxes represent the sum in quadrature of statistical and systematic errors, and the bars indicate the statistical errors only. The curves are the results of the fit by with the two functions described in the text. (Right) Comparison of measured spectrum with those generated in a PYTHIA and in a PHOJET sample, normalized to the same integral in the measured  $p_T$  range (0.7 to 3 GeV/c).

To obtain the yields, the  $\phi$  reconstruction efficiency was determined by a PYTHIA simulation made with a realistic implementation of the ALICE detector (see fig. 2, right). Finally, the corrected counts were normalized to the total number of inelastic collisions.

Two main sources of systematic error were identified: one was related to the choice of the function for the background subtraction, and another to TPC cuts ( $dE/dx$  and number of clusters). They were estimated to range between 0.4 to 5.6% in the first case and from 0.9 to 6% in the second one, depending on  $p_T$ . They are smaller than the statistical error which ranges between 10% and 20% due to the sample size.

**3.3. Results.** – Figure 3 (left) reports the corrected  $p_T$  spectrum. It was fitted with an exponential function and with a Levy/Tsallis function [5], which in general reproduces better the power-law tail at large momenta. The  $dN/dy$  was computed by integrating the fit functions in the 0–0.7 GeV/c and 3– $\infty$  GeV/c  $p_T$  ranges and adding the sum of measured counts in the region between  $p_T = 0.7$  and 3 GeV/c which turned out to correspond to 52% of the total. For both cases the average transverse momentum was also computed. Table I reports the computed yields and mean  $p_T$ . As expected, the two functions return different values for the latter, due to the very different contribution coming

TABLE I. –  $dN/dy$  and mean  $p_T$  from the spectra fit (see text). First and third lines refer to function integration, second line gives the integral yield in the measured  $p_T$  range.

Integral	Levy			%	Exponential			%
0–0.7 GeV/c	0.0090	$\pm$	0.0007	45	0.009	$\pm$	0.002	47
0.7–3 GeV/c	0.0104	$\pm$	0.0007	52	0.0104	$\pm$	0.0007	52
3– $\infty$ GeV/c	0.0006	$\pm$	0.0001	3	0.0002	$\pm$	0.002	1
Total	0.020	$\pm$	0.001	100	0.020	$\pm$	0.002	100
$\langle p_T \rangle$ (GeV/c)	0.98	$\pm$	0.07		0.88	$\pm$	0.06	

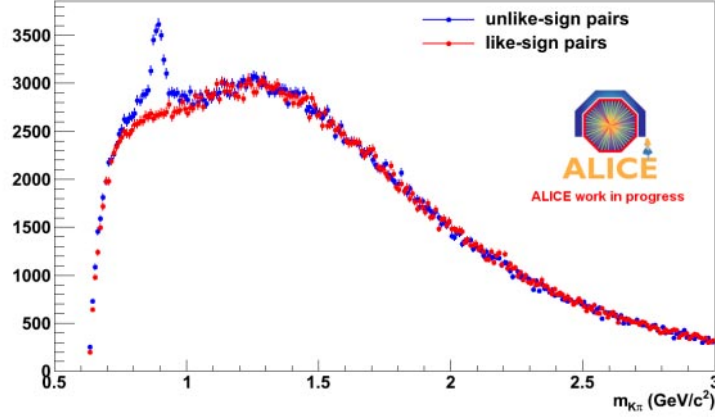


Fig. 4. – (Colour on-line)  $K\pi$  invariant mass spectra for the extraction of the  $K^*(892)$  resonance in pp collisions at the c.m. energy of 7 TeV ( $p_T$ -integrated). The blue histogram is built with all the unlike-sign pairs, where the peak is well visible, while the other refers to like-sign pairs and is used to subtract the combinatorial background.

from the high momentum tail. Figure 3 (right) reports a comparison of the measured points with PYTHIA and PHOJET. Both Monte Carlo spectra were normalized to the same integral in the measured region (0.7 to 3 GeV/c), and while in this range they appear to be quite compatible, PHOJET gives a larger yield in the extrapolation region at low  $p_T$ .

#### 4. – Results at 7 TeV

The sample of pp collision data at 7 TeV has a very large statistics (up to 700 million events taken during 2010 run). This allowed one to face the study of those resonances with a low signal/background ratio (*e.g.*, the  $K^*(890)$  through the charged  $K\pi$  decay channel) or with a low efficiency for retrieving their daughters (*e.g.*, the  $\Sigma(1385)$  through the  $\Lambda + \pi$  decay channel).

Figure 4 shows a result on the extraction of the  $K^*(892)$  invariant mass peak from a sample of 17 million pp minimum-bias events at 7 TeV: in this case, the background was estimated from the invariant mass distribution of like-sign pairs. Figures 5 and 6 show the  $\Lambda\pi$  invariant mass distribution for the extraction of the  $\Sigma(1385)$ , computed with 76 million minimum-bias events at the same energy as above. In this case, the background was reproduced by a 3rd-order polynomial fit outside the peak range, and then subtracted.

The very large statistics obtained will allow one to measure the  $\phi(1020)$  resonance with a  $p_T$  binning much finer than it was possible to do with the sample at 900 GeV. A small sample (about 10 million events) of 7 TeV pp data has been analyzed in order to extract the  $\phi$   $p_T$  spectrum. The analysis was carried out using essentially the same strategy adopted for the 900 GeV sample. Moreover, in this case, the analysis included also the tracks which were reconstructed in the ITS stand-alone using all clusters rejected after the global tracking. This is expected to help in recovering about 10% of the tracks which were lost due to TPC dead zones or to their low transverse momentum ( $\leq 200$  MeV/c).

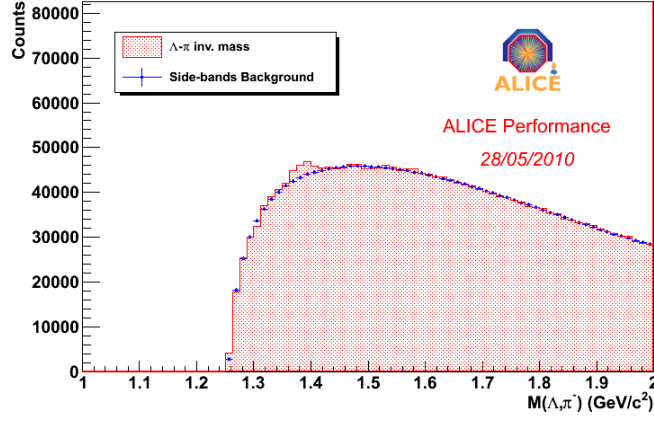


Fig. 5. –  $\Lambda\pi$  invariant mass spectrum for the extraction of the  $\Sigma(1305)$  resonance in pp collisions at the c.m. energy of 7 TeV ( $p_T$ -integrated). The filled histogram is a polynomial description of the background fitted outside the peak range.

Figure 7 shows a performance plot where one can clearly see the resonance peak in several small  $p_T$  bins, down to 400 MeV/ $c$ .

## 5. – Conclusions

We have shown the analysis of  $\phi(1020)$  resonance in ALICE obtained with the first LHC data from pp collisions at 900 GeV and preliminary results on  $\phi(1020)$ ,  $K^*(892)^0$  and  $\Sigma(1385)$  measurements with the 2010 LHC data from pp collisions at 7 TeV. The 900 GeV analysis is completed and  $dN/dy$  and  $\langle p_T \rangle$  were measured for the first time for the  $\phi$ . QCD-inspired models reproduce quite well the  $\phi(1020)$   $p_T$  spectral shape, even if

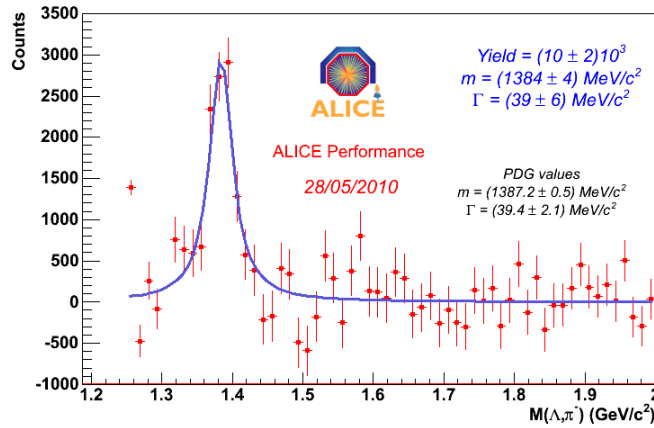


Fig. 6. –  $\Lambda\pi$  invariant mass spectrum after background subtraction, fitted by means of a Breit-Wigner function.

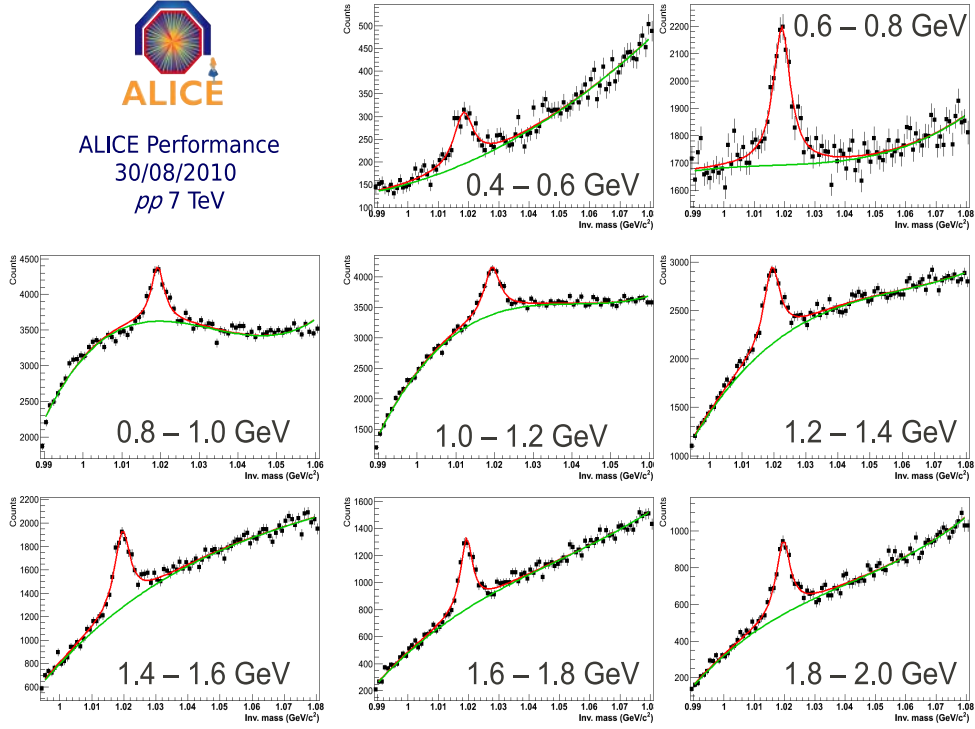


Fig. 7. –  $K^+K^-$  invariant mass distribution in several  $p_T$  bins in pp collisions at the c.m. energy of 7 TeV (bin sizes in GeV/c). In all plots, the signal is well visible over the background and a fit is performed using the combination of a 3rd-order polynomial background and a Breit-Wigner function for the peak.

they differ in their predictions at low momenta, where the low statistic available for this analysis prevents one from drawing more detailed conclusions. All preliminary results from data at 7 TeV look very promising, and demonstrate the excellent PID performances of the ALICE detector and its capabilities for resonance study.

## REFERENCES

- [1] ALICE COLLABORATION, *JINST*, **3** (2008) S08002.
- [2] MARKERT C. *et al.*, *Phys. Lett. B*, **669** (2008) 92 and references therein.
- [3] STAR COLLABORATION, *Phys. Lett. B*, **612** (2005) 181; *Phys. Rev. C*, **79** (2009) 064903.
- [4] ALICE COLLABORATION, arXiv:1012.3257v2 [hep-ex] (2011).
- [5] TSALLIS C., *J. Stat. Phys.*, **52** (1988) 479.